

Ferromagnetic Resonance Linewidths in Ultrathin Structures; Theoretical Studies of Spin Pumping

A. T. Costa¹, Roberto Bechara Muniz² and D. L. Mills³

¹ Departamento de Ciências Exatas
Universidade Federal de Lavras
37200-000 Lavras, M. G. Brazil

² Instituto de Física
Universidade Federal de Fluminense
24210-340 Niterói, R. J. Brazil and

³ Department of Physics and Astronomy, University of California, Irvine, CA 92697, U. S. A.
(Dated: April 14, 2024)

We present theoretical studies of the spin pumping contribution to the ferromagnetic resonance linewidth for various ultrathin film ferromagnetic structures. We consider the isolated film on a substrate, with Fe on Au (100) and Fe on W (110) as examples. We explore as well the linewidth from this mechanism for the optical and acoustical collective modes of FM/Cu_N/FM/Cu (100) structures. The calculations employ a realistic electronic structure, with self-consistent ground states generated from the empirical tight-binding method, with nine bands for each material in the structure. The spin excitations are generated through use of the random phase approximation applied to the system, including the semi-infinite substrate on which the structure is grown. We calculate the frequency response of the system directly by examining the spectral density associated with collective modes whose wave vector parallel to the surface is zero. Linewidths with origin in leakage of spin angular momentum from the adsorbed structure to the semi-infinite substrate may be extracted from these results. We discuss a number of issues, including the relationship between the interfilm coupling calculated adiabatically for trilayers, and that extracted from the (dynamical) spin wave spectrum. We obtain excellent agreement with experimental data, within the framework of calculations with no adjustable parameters.

PACS numbers: 76.50.+g, 75.75.+a, 72.25.Mk

I. INTRODUCTORY REMARKS

The damping of spin motions in nanoscale ferromagnetic structures has been a topic explored actively in recent years. The interest focuses on the 3d transition metal ferromagnets and their alloys, since one may now synthesize diverse ultrasmall magnetic structures of very high quality from them. It is the case as well devices are fabricated from these materials, in which ferromagnetism is realized even well above room temperature. It is very clear that one encounters damping mechanisms not present in the bulk crystalline form of the constituents. That this is so has been evident for many years now¹. The primary question then centers on the origin of the new damping mechanisms operational in nanomagnetic structures.

Of course, the electronic structure of such entities may differ substantially from that in the bulk crystalline matter, by virtue of distortions of the lattice associated with the mismatch in lattice constant between the film and the substrate. In addition, a large fraction of the moment bearing ions sit at interfaces or on surfaces, and this will influence the electronic structure as well. Hence, if the Gilbert damping constant G is used as a measure of the damping found for long wavelength spin motions, one may expect intrinsic differences between the values of G appropriate to nanoscale structures, and that appropriate to bulk materials.

It is now very clear from diverse experimental studies that the damping mechanisms operative in ultrathin ferromagnets do not have their origin only in differences between the electronic structure of bulk and nanoscale matter. Evidently distinct new mechanisms are present. For instance, an earlier analysis of data on ferromagnetic resonance (FMR) linewidths show a dependence on growth conditions whose influence on electronic structure is surely rather indirect¹. A few years ago, it was argued² that a mechanism referred to as two magnon damping can be activated by defects on the surface or at interfaces. The density and character of such defects is clearly influenced by the manner in which the film is grown. The theory of two magnon damping makes explicit predictions regarding the frequency variation of the linewidth and its dependence on the orientation of the magnetization^{2,3}. Also, Rezende and his colleagues have demonstrated that it accounts quantitatively for the strong wave vector dependence found upon comparing linewidths measured in FMR, and those measured in Brillouin light scattering (BLS)⁴. We refer the reader to a review article which describes the theory of two magnon damping in ultrathin ferromagnetic films, and the experimental evidence for its presence⁵.

Two magnon damping is an extrinsic mechanism activated by defects on or within an ultrathin film. In the

recent literature, experimental evidence has been presented for the presence of a mechanism operative in ultrathin ferromagnetic Im structures which is intrinsic in character^f. It should be remarked that Berger⁷ and Slonczewski⁸ predicted this mechanism should be present in ultrathin Im s in advance of the experiments. Suppose we consider an ultrathin Im of a ferromagnetic metal placed on a metallic substrate. The magnetic moments in an ultrathin ferromagnetic Im are embedded in a sea of conducting electrons which, of course also have spins and magnetic moments. As the magnetic moments are excited in an FMR or BLS experiment, they precess coherently. Angular momentum is transferred to the conduction electrons, and this is transported across the interface between the Im and the substrate in the form of a spin current. Thus, spin angular momentum is lost from the ferromagnetic Im , and the spin motions are damped as a consequence. This source of damping is referred to as the spin pumping mechanism. As the ferromagnetic Im is made progressively thicker, the spin pumping contribution to the linewidth decreases roughly inversely with the Im thickness, according to theory. This behavior is found in the experimental data.

By now, numerous theoretical descriptions have been given for the spin pumping contribution to the linewidth. In the early papers cited in the previous paragraphs^{7,8} a simple phenomenological picture of the ferromagnetic metal and the surrounding materials is employed. The magnetic moments are described as localized moments, with $s(\mathbf{l})$ the spin angular momentum associated with lattice site \mathbf{l} . Such local moments are assumed to be coupled to a conduction electron bath, modeled as free electrons in quantum wells. These interact with the local moments via the classical $s\mathbf{l}$ exchange interaction $\mathbf{J}S(\mathbf{l}) \cdot \mathbf{s}$, with \mathbf{s} the conduction electron spin. Within such a framework, general features of the spin pumping mechanism may be elucidated, but quantitative predictions for specific materials are not contained in such simple descriptions.

Within such a framework, Simanek and Heinrich⁹ introduced an elegant picture of the origin of the spin pumping contribution to the linewidth. A ferromagnetic Im with static magnetization placed in contact with a nonmagnetic metal induces RKKY spin oscillations in the nonmagnetic material. If the magnetization of the ferromagnet precesses at a finite frequency, the RKKY oscillations do not quite follow the magnetization of the substrate. In essence, the RKKY coupling is frequency dependent. If the frequency dependent RKKY interaction is expanded in powers of the frequency, the lowest order linear term in the effective equation of motion of the magnetization provides a contribution to the effective damping constant felt by the ferromagnetic spins. In Ref. [9], only a single layer of localized spins was considered, embedded within an electron gas. One of the present authors has elaborated on this basic scheme by considering N layers of local moments to simulate a multilayer Im , with conduction electrons described by a quantum well picture¹⁰. A prediction which emerges from this model is that the spin pumping contribution to the linewidth does not fall off simply like $1/D$, with D the thickness of the ferromagnetic Im . Quantum oscillations are superimposed on this $1/D$ falloff. Further discussion of this approach has been presented by Simanek¹¹.

A rather different approach has been taken by Tserkovnyak and his colleagues². These authors use a one electron picture, in which the electron wave functions extend over the entire structure considered, the ferromagnetic Im and the nonmagnetic metals which are in contact with it. Spin precession within the ferromagnetic Im is introduced by virtue of a postulated form for a time dependent density matrix. The flow of spin angular momentum out of the ferromagnetic Im in the presence of the spin precession is described in terms of the transmission and reflection coefficients associated with appropriate scattering states. Recently a study by this group has appeared where density functional electronic structure calculations are employed to calculate spin pumping contributions to the linewidth for specific material combinations³. The agreement with experimental data which follows from this analysis is very good, though we note that the theory explores an ultrathin ferromagnetic Im bounded on both sides by a semi-infinite nonmagnetic metal, a structure quite different than employed in the actual experiments. The authors conclude that the oscillations found within the quantum well model of Ref. [10] are in fact very modest in amplitude when a proper electronic structure is employed. We remark that in the series of calculations which motivate the present paper, we find similar results.

In this paper, we address the calculation of spin pumping linewidths for various ultrathin Im /substrate combinations by a method quite different than found in the studies cited above. We calculate directly the full frequency spectrum of the response of diverse structures to applied microwave fields whose wave vector parallel to the surfaces of the structures is zero, within the framework of a method which provides a realistic description of the electronic structure of the sample of interest. We extract linewidths by fitting the lines in the absorption spectra with a Lorentzian, very much as done in experimental analyses of actual data. As remarked above, we note that the formalism employed by the authors of Ref. [12] and Ref. [13] requires the ferromagnetic Im to be bounded on both sides by nonmagnetic metals of semi-infinite extent, since the reflection and transmission coefficients required are found from scattering states associated with electrons reflected from and transmitted through the ultrathin ferromagnetic Im . Our method allows us to address the more realistic case of an ultrathin Im adsorbed on a semi-infinite substrate, bounded by vacuum (or if we wish a capping layer) on the other side. As we shall demonstrate below, we can also calculate the linewidths of trilayers adsorbed on a semi-infinite substrate, so we can study the linewidth of both the acoustic and optical spin wave modes. Such structures have been explored by the Babelschke group¹⁴. While, for reasons discussed below, it is difficult to make a detailed comparison between our results and their data, we do see features in our re-

$\omega_a(\mathbf{Q}_k)$ be the frequency of one such mode, and let $\mathbf{e}_a(\mathbf{Q}_k; \mathbf{l}_\perp)$ be the associated eigenvector. For this model, which we note is inappropriate for the itinerant electron ferromagnetic films considered here^{15,16,18}, one may show that

$$A(\mathbf{Q}_k; \mathbf{l}_\perp) = \sum_a \mathbf{e}_a(\mathbf{Q}_k; \mathbf{l}_\perp)^2 \left(\omega_a(\mathbf{Q}_k) \right) \quad (3)$$

The form in Eq. (3) provides one with an understanding of the information contained in the spectral density function.

Of course, it would be highly desirable to base the analysis of the spin dynamics of systems such as we explore through use of a state of the art density functional description of the ground state, combined with a time dependent density functional analysis (TDDFA) of the spin fluctuation spectrum. At the time of this writing, one cannot carry out studies of the spin fluctuation spectrum within the TDDFA for systems as large as we have studied in the past^{15,16} and that we explore in the present paper. The demands on computation time are prohibitive. We believe it is essential to employ fully semiconducting substrates for proper calculations of spin wave linewidths with origin in decay of the collective excitations to the Stoner excitation manifold. One must have a true continuum of final states for a proper description of the linewidth. All of our calculations employ a full semiconducting substrate, unless otherwise indicated. The virtue of our multiband Hubbard model is that once the irreducible particle hole propagator is computed, inversion of the RPA integralequation is straightforward and fast, by virtue of the fact that the particle-hole vertex is separable in momentum space within our framework. TDDFA calculations employ an ab initio generated vertex function which requires the numerical solution of a full integralequation, once the irreducible particle hole propagator is in hand. One can handle only rather small systems within this framework, at present.

If one describes our treatment of the ground state and then the RPA description of the spin dynamics by Feynman diagrams, it is the case that we include the same set of diagrams as incorporated into the full density functional theory, so in a certain sense one may view what we do as a simplified version of time dependent density functional theory. However, technical simplifications such as those described in the previous paragraph enable us to address very large systems. We note that our calculations involve no adjustable parameters, since all of our input parameters are taken from the appropriate literature. A rather detailed discussion of how we proceed is contained in Ref. [19], and considerable detail is found in the first paper cited in Ref. [15].

In spite of the remarks above, it is the case that the numerical work involved in the calculation of the dynamical susceptibility is extremely demanding from the computational point of view. As discussed in detail in the first paper cited in Ref. [15], to calculate the irreducible particle hole propagator it is necessary to calculate an energy integral whose integrand is itself a two dimensional integral over the full surface Brillouin zone. We have also shown that very careful attention must be paid to convergence of the Brillouin zone integrations for physically reasonable results to emerge from $\chi''(\mathbf{l}_\perp; \mathbf{l}_\parallel^0)$. We refer the reader to Fig. 6 of the first paper in Ref. [15] and the associated discussion in the text. We find that 4224 points in the surface Brillouin zone must be employed to insure proper convergence. The irreducible particle hole propagator is a matrix structure, whose size is the number of layers in the film, N , times the number of orbitals included in the calculation. Thus, for us to analyze spin fluctuations in a 10 layer ferromagnetic film, we must perform the Brillouin zone integration just described for a 90×90 matrix. For films deposited on semiconducting substrates, of course we require the single particle Green's function for the semiconducting structure. This part of the computation also consumes a considerable fraction of the total computing time.

Fortunately, the problem in question can be easily adapted to run in parallel on a cluster of workstations. We adopted a very straightforward parallelization strategy, in which we spread 64 points of energy integration among 32 processors. For interprocess communication, we use the MPICH implementation²⁰ of the Message Passing Interface (MPI)²¹. The interprocess communication overhead for this specific problem is minimal, so that the execution time scales roughly linearly with the number of processors. This allows us to calculate the dynamic susceptibility of relatively thick ferromagnetic films (15 layers) on a fully semiconducting substrate, in a relatively short time. A computation of the frequency response for one film can be performed in less than 48 hours. Typically to generate the absorption spectra shown in section III, we use one hundred frequencies.

III. RESULTS AND DISCUSSION

In our previous studies of spin waves in various ultrathin film/substrate combinations, our emphasis was on excitations with relatively large wave vectors. The excitation energies of such modes are very large compared to the Zeeman energy, which describes the interaction of the spins in the system with externally applied field. Thus the external field was taken to be zero in all of our previous studies. Here, when we examine the modes whose wave vector is identically zero, with emphasis on the modes seen in FMR experiments, quite clearly we must incorporate the externally applied magnetic field. In the results that follow, we have immersed all the electrons in a spatially uniform Zeeman field, and we denote the precession frequency in this Zeeman field by ω_0 .

We should say a few words about how the strength of the Zeeman field has been chosen. First of all, the energy scale used in our electronic structure is the electron volt, or equivalently the Rydberg. The spin excitations we studied in our earlier papers had energies compatible with this scale, in the range of 0.01 eV to 0.3 eV^{15,16} depending on the wave vector we chose to study. If we choose our applied Zeeman field to be in the range actually used in laboratory experiments, then the energy scale of the FMR mode is so small ($\sim 10^{-5}$ eV) that an enormous amount of computation time would be required to produce calculations with an energy grid so fine as to allow us to generate accurate profiles for these very low energy modes. It is the case, however, that so long as ω_0 is very small compared to the typical electronic energy scales, the linewidths scale linearly with resonance frequency. We remark that we have checked carefully that this is so, in our early studies. So long as we remain in the regime where the linewidth scales in this linear manner, we may choose an unphysically large value for ω_0 , and scale the computed linewidths appropriately when we compare our results with data. What we choose to do instead is always to plot the ratio ω_0/ω_r , with ω_r the linewidth determined as discussed below. This is independent of applied field, in the regime where the linearly scaling holds. In the calculations to be presented in this paper, we have chosen $\omega_0 = 2 \times 10^{-3}$ Rydbergs = 27 meV.

In Fig. 1(a), we show the absorption spectrum for the FMR mode (the lowest lying spin wave mode of the Fe_{12} , with wave vector parallel to the Fe_{12} surface identically equal to zero) of a two layer Co_{12} adsorbed on the $\text{Cu}(100)$ surface. One sees the resonance line, with peak very close to ω_0 . In principle, there can be a g shift associated with this mode even in the absence of spin orbit coupling, since strictly speaking the amplitude of the spin motion in the direction normal to the surface is not perfectly uniform. In our earlier studies of the electron spin resonance response of isolated magnetic adatoms adsorbed on the $\text{Cu}(100)$ surface, we found such g shifts to be quite large. Here we find that the peak of the absorption line coincides exactly with ω_0 , so far as we can tell.

There is another idealization we have made that must be mentioned. In an actual sample, where a ferromagnetic Fe_{12} is on top of a nonmagnetic substrate such as Cu , when the spins precess in the ferromagnet, dynamic dipolar fields are generated by the spin motion. Thus, for a Fe_{12} magnetized parallel to its surfaces, the FMR frequency is shifted from $\omega_0 = H_0$ to $[H_0(H_0 + 4 M_s)]^{1/2}$, where γ is the gyromagnetic ratio for the ferromagnetic Fe_{12} , H_0 is the applied Zeeman field, and M_s is the saturation magnetization. It is also the case that the gyromagnetic ratio for the ferromagnetic Fe_{12} will differ from that of the conduction electrons in the substrate. Thus, in an actual sample, the precession frequency of the spins in the ultrathin ferromagnetic Fe_{12} will differ from that for electrons in the substrate. We have explored the influence of this effect by varying the ratio of the Zeeman frequency of the spins in the ferromagnet, to that of the spins in the substrate by as much as a factor of two. We find that our linewidths, normalized to the resonance frequency in the ferromagnet, are insensitive to this difference. On physical grounds one expects this. In microscopic language, the linewidths we calculate have their origin on the transfer of angular momentum from the coherently precessing moments in the ferromagnet to the bath of itinerant band electrons. If we think of this as a form of Landau damping, where the spin wave decays to the bath of Stoner excitations of the Fe_{12} /substrate complex (spin triplet particle hole excitations), a shift in the precession frequency of the ferromagnetic Fe_{12} relative to that of the substrate electrons is compensated by a very tiny shift in the wave vector transfer involved in the decay process, on the scale of the relevant two dimensional Brillouin zone. Note that wave vector components normal to the surface are not conserved for the systems we study. Thus, in Fig. 1(a) and in the results to be discussed below, all electrons in the system are subjected to the same external field, and are assumed to have the same gyromagnetic ratio, with dipolar fields in the ferromagnet ignored.

In Fig. 1(b), we show calculations of the of a $\text{Co}_2\text{Cu}_2\text{Co}_2$ trilayer adsorbed on a semiconducting $\text{Cu}(100)$ surface. One now sees two modes, the acoustical and the optical spin wave mode of the ferromagnetic bilayer. It is clear from visual inspection that the acoustical mode is narrower than the FMR line shown in Fig 1(a), while the optical mode is substantially broader, a pattern seen in experimental studies of such systems¹⁴. It should be noted that in Fig. 1(b), it is not quite the FMR absorption spectrum that is displayed. For two such identical Fe_{12} s, the antisymmetric optical spin wave mode has no net transverse magnetic moment, and thus would be silent in an FMR spectrum. In actual FMR experiments where both modes are observed, the two ferromagnetic Fe_{12} s are inequivalent. What we display in Fig. 1(b) is the spectral density function $A(\omega_k = 0; \parallel; 1)$, where we have taken $\mathbf{k} = 1$, where the 1 refers to the outermost layer of the outermost Fe_{12} . The physical interpretation of this spectral density function is that it describes the frequency spectrum of the fluctuations of the spins in the atomic layer indicated, at zero wave vector parallel to the surface. The acoustic and optical spin wave both leave their signature on this response function.

One final remark is that our procedure for determining the linewidths discussed below is as follows. For each structure of interest, we calculate a spectrum such as that illustrated in Fig. 1(a) and Fig. 1(b). Then we fit the curves to appropriate Lorentzians, and from this we extract a linewidth. The quantity $\omega_{1/2}$ is the half width at half maximum.

The first case we discuss is that of Fe_{12} s adsorbed on the $\text{Au}(100)$ surface. This is the system studied by Urban, Woltersdorf and Heinrich⁶.

In Fig. 2, we show our calculated linewidths as open circles, for Fe_{12} thicknesses in the range of two to ten monolayers. The solid line is a best power law fit to the data, which turns out to be $1/(N_{\text{Fe}})^{0.98}$ law, with N_{Fe} the

number of Fe layers. Various authors^{7,8,12} have argued that the spin pumping linewidth should fall off inversely with the thickness of the ferromagnetic film, so these results are consistent with this picture. Our calculations show this behavior nicely. For small thicknesses, we see oscillations of modest amplitude around the $1/N_{\text{Fe}}$ law. These are quantum oscillations such as those discussed in Ref. [10], though as discussed by the authors of Ref. [13] the simple quantum well model exaggerates their amplitude.

The solid circles in Fig. 2 are data taken from Ref. [6]. Theory and experiment agree very nicely. Unfortunately it is difficult for us to carry out calculations for films much thicker than ten layers for the FMR mode. In our integrations over energy, a small imaginary part is added to energy denominators, and we must always keep this small compared to the linewidth. We must decrease this as the film gets thicker, and at the same time we must increase the density of points in our integration grids to generate a reliable, converged line shape uninfluenced by the numerical procedures.

It is interesting to inquire how the linewidth depends on the electronic structure of the substrate. To explore this, we have carried out calculations for an Fe film deposited on the W (110) surface. While we are unaware of any FMR studies of this system, the magnetism associated with the Fe/W (110) system has been extensively studied in the literature. Our results are given in Fig. 3. The straight line is a best fit to a power law dependence on the Fe film thickness, and in this case we find $1/(N_{\text{Fe}})^{0.81}$, just a bit slower than a simple variation inversely proportional to the film thickness. However, we again see quantum oscillations about a simple power law fit, at smaller thickness, so a simple power law is a bit of an oversimplification. Surprisingly, in our view, the numerical values of the linewidths displayed in Fig. 3 are not so very different than those in Fig. 2. We had expected larger linewidths, because of the large density of states in the substrate associated with the unfilled d bands of W. It should be pointed out, however, that the connectivity of an Fe film is larger when it is adsorbed on Au(100) than when it is adsorbed on W (110). An Fe atom at the interface with the Au(100) surface is connected to four nearest neighbor Au atoms, whereas it is coupled to just two nearest neighbor W atoms in the Fe/W (110) interface. One virtue of our empirical tight binding approach is that we can probe the physics responsible for results such as these by artificially selecting parameters. We turn to such studies next, to obtain insight into this result.

It is interesting to compare the calculated linewidths for an Fe film adsorbed on W (110), and for an identical film adsorbed on a bcc Cu crystal, which we can simulate with our approach. Here the connectivity to the substrates is the same. Of course, in the first case the Fermi level intersects the d band complex of the substrate, whereas in the second case the d bands are well below the Fermi level. For the cases of a two layer Fe film on W (110) we see from Fig. 3 that γ_0 assumes the value 1.8×10^{-2} , whereas for the Fe film on Cu (110), the line is actually a bit broader, with $\gamma_0 = 2.7 \times 10^{-2}$. Even though the two numbers are rather close to each other, it would seem that the physics which underlies the transfer of spin angular momentum across the interface is rather different in the two cases. In Fig. 4, we show calculations which illustrate this. Let us first look at the right panel, the case of Fe on W (110). The solid curve is the spectral density calculated with use of the full electronic structure. The dashed curve is a calculation in which the d-d hopping terms are set to zero across the interface. The line narrows very substantially when the d-d hopping is shut off, as we see. Evidently for this case, direct communication between the d electrons in the Fe film and the W substrate plays a central role in the transfer of spin angular momentum. The electrons at the W Fermi surface have strong d character, and the electrons in the Fe with strong sp character play a minor role in the damping process. This view is reinforced by the dot dash curve in the right hand panel of Fig. 4, where the sp hopping terms are set to zero across the interface. We see little change in the spectral density. The situation is very different for the case of Fe on Cu (110), as we see from the left hand panel in Fig. 4. We see here that communication between both the sp and the d like portions of the electronic wave function across the interface play an important role. Even though the 3d bands of Cu are completely filled, there is d character admixed in the electron wave functions in the vicinity of the Fermi energy, while at the same time coupling through the sp character of the wave function enters as well. Thus, while the final numbers for the spin pumping contributions to the linewidth are rather similar for these two very different substrates, the physical picture which underlies the transfer of spin angular momentum across the interface is rather different. In view of this discussion, it would be of great interest to see experimental FMR linewidth studies for the case of Fe on W (110).

We turn next to a discussion of our calculation of linewidths of the FMR modes of ferromagnetic/nonmagnetic metal/ferromagnetic film combinations adsorbed on semiconducting substrates. We have already seen that such structures produce two features in the absorption spectrum, one from an acoustic spin wave mode, and one from an optical mode. The splitting between these two modes is controlled by the well known interfilm exchange coupling transmitted through the nonmagnetic spacer layer. As remarked above, if one has a sample with two identical ferromagnetic films, only the acoustical mode is active in an FMR experiment, since the optical mode possesses no net transverse magnetic moment. In samples fabricated from ultrathin films, the thickness of the trilayer is small compared to the microwave skin depth, so to excellent approximation the films are illuminated by a spatially uniform magnetic field. We note that in Brillouin light scattering, one may observe both modes, since the optical skin depth is in the range of 10-20 nm for materials of current interest. Here, the exciting optical field is spatially non uniform, on the length scale of the structure. It is the case, though, that in any real sample, the two films will always be inequivalent even if

their thicknesses are the same. For instance, both interfaces of the innermost In are in contact with non magnetic metals, with the substrate on one side and the spacer layer on the other. The outer In has vacuum on one side, and the spacer layer on the other. Hence, the anisotropy fields will be different in each In , and this will render them inequivalent. As discussed below, we have simulated such effects by applying different external magnetic fields to each In . First, however, we present our results for the case where the two ferromagnetic In s are regarded as identical in character.

Before we turn to our results, we remark on how we proceed with our determination of the linewidths for the optical and the acoustical mode of the trilayer structure. In Fig. 1(b), we show the spectral density function for a case where the Cu spacer layer is sufficiently thin that the two modes can be resolved easily in the spectral density associated with one selected layer. As the Cu spacer is made thicker, the splitting between the two modes decreases and if we plot the spectral function illustrated in Fig. 1(b), we simply see a single asymmetric line, with the optical mode buried in the wing of the acoustical mode. We have proceeded as follows. For each frequency, we form a two by two matrix with elements $\epsilon_{11} = \sum_{l_2, l_2^0} \text{Im} f_{+; (0; l_2; l_2^0)}^2$, $\epsilon_{12} = \sum_{l_2, l_2^0} \text{Im} f_{+; (0; l_2; l_2^0)} g$ and so on. In

the definition of ϵ_{11} , the sums on both l_2 and l_2^0 range over the atomic planes in the outermost In , while in ϵ_{12} the sum on l_2 ranges over the atomic planes of the outermost In , and the sum over l_2^0 ranges over the atomic planes of the innermost In . Diagonalization of this matrix at each frequency leads us to two eigenvectors, one with acoustical character and one with optical character. If we generate plots of the spectral densities of these two characteristic motions, in one we see only the acoustical feature, and in the second we see only the optical feature. We illustrate this in Fig. 5. In Fig. 5(a) we show the spectral density function associated with spin fluctuations in the innermost In of a $\text{CoCu}_4\text{O}_2/\text{Cu}(100)$ structure. The optical mode appears in the wing of the acoustical mode, and one cannot reliably extract a width for the mode from this response function. In Fig. 5(b) we see how one may isolate the acoustical mode by the procedure just describe, and in Fig. 5(c) we show the optical mode.

We remark that for the samples studied experimentally in Ref. [3], the two ferromagnetic In s in the trilayer have very different resonance frequencies when taken in isolation, so the issue of discriminating between the two modes did not arise. Save for one measurement discussed below, the trilayer structures studied in Ref. [3] may be viewed as two oscillators whose resonance frequencies differ by an amount much larger than their linewidths, coupled weakly by the inter In exchange coupling mediated by the spacer layer.

In our earlier studies of large wave vector spin waves and their dispersion¹⁶ we have compared the dispersion relation which emerges from our dynamical theory with that calculated on the basis of adiabatic theory, where exchange couplings between spins are calculated within quasi static theory, and a Heisenberg Hamiltonian constructed from these is used to generate a spin wave dispersion curve. We found substantial differences between the two cases. The strong damping present at large wave vectors leads to shifts in the frequency of the spin wave. This effect, which softens the modes, is not contained in calculations based on an adiabatic description of energy changes associated with rotations of the moments. One can inquire if the effective inter In exchange couplings deduced from the splitting between the acoustical and optical spin wave modes of the trilayer are the same as those described by adiabatic theory.

We provide a comparison which addresses this issue in Fig. 6. The solid line shows the dependence of the inter In coupling strength on N , the number of Cu layers between the two Co_2 In s, calculated adiabatically using the method in Ref. [23]. The dashed line provides the results deduced from the splitting between the two spin wave modes of the structure. The two agree rather well, though there are indeed small differences between the two.

It is evident that we find the width of the optical mode of the trilayer significantly larger than that of the acoustic mode. This is consistent with the results reported in Ref. [14], as noted earlier. Very interesting to us is the data in Fig. (6) of Ref. [14], where the linewidth measured for these two modes is given as a function of the number of Cu layers between the two ferromagnetic In s. One sees very clear quantum oscillations in these two linewidths. In our Fig. 7, we show calculations of the variation of the acoustic and optical mode linewidths with N , the number of Cu spacer layers in our $\text{Co}_2\text{Cu}_N\text{Co}_2/\text{Cu}(100)$ structure. The calculations reproduce the features found in the data strikingly well. For instance, in our calculations we see a peak in the linewidth of the acoustic mode at six atomic layers of Cu and a second somewhat smaller peak at nine layers. Both features appear in the data, indeed with the peak at six layers the most prominent. Also very much as in the data, for the optical mode we see the peak at six layers in our calculations, while the peak at nine layers is suppressed strongly. In our calculations, the optical mode linewidth, reckoned relative to that of the acoustic mode, is larger than that in the data. At the peak at six layers, we

find the width of the optical mode larger than that of the acoustical mode by a factor of roughly five, whereas in the data this ratio is a bit less than a factor of two. A direct comparison of this ratio with the data is not so relevant in our minds, since the resonance frequencies of our two Co_2 In s (each taken in isolation) are identical, whereas that of the $\text{Co}_{1.8}$ In and the Ni In used in Ref. [14] are different.

Some of the data in Ref. [14] has been taken on $\text{Ni}_3\text{Cu}_N\text{Ni}_3/\text{Cu}(100)$ samples. The resonance frequencies of the Ni_3 and Ni_3 In s differ substantially when the externally applied field is in plane, presumably because of the proximity of these Ni In s to the spin reorientation transition. However, the authors of Ref. [14] were able to sweep

the resonance frequency of one Mn through the second by varying the angle of the external applied magnetic field with respect to the plane of the Mn s. They argue that the linewidths of the two modes approach each other when the resonance frequencies coincide. This is illustrated in their Fig. 4, for a sample with $N = 12$. For such a thick copper spacer layer, the inter Mn exchange coupling is negligible.

We can simulate this with our $\text{Co}_2\text{Cu}_N\text{Co}_2/\text{Cu}(100)$ structures by applying a different magnetic field to each Mn . In Fig. 8 we present results of a study where the resonance frequency of the outer Mn is ω_0 and that of the inner Mn is ω_1 , where ω_1 is varied from 1 to 2. By varying ω_1 , we can study how the linewidth of each mode behaves if the two Mn s initially are detuned ($\omega_1 = 2$), and then brought to the point where the isolated Mn resonance frequencies coincide ($\omega_1 = 1$). Our calculations are carried out for $N = 10$, where the inter Mn exchange coupling is very weak.

We presume the authors of Ref. [14] have fitted their FMR spectra to a sum of two Lorentzians in order to extract the width of the two modes. We have attempted a similar procedure with simulations of the FMR absorption spectrum of the structure. However, we find that when ω_1 is fairly close to unity, we cannot reliably extract linewidths for the two modes by fitting the overall spectral density in this manner. In Fig. 8(a), the solid line shows the absorption spectrum of the trilayer for the case where $\omega_1 = 1.2$, and we see the high frequency mode as a barely perceptible feature on the high frequency side of the line. The solid line is the function $a(\omega) = \frac{P^1}{P^1 + P^2} \text{Im} f + \frac{P^2}{P^1 + P^2} \text{Im} f + \frac{P^3}{P^1 + P^2} \text{Im} f$; $(0; \frac{1}{2}; \frac{1}{2})g$. $\frac{P^1}{P^1 + P^2} = 1, \frac{P^2}{P^1 + P^2} = 1$

This gives the absorption spectrum of the trilayer, if it is illuminated by a spatially uniform microwave field. Also in Fig. 8(a), we give the absorption spectrum for the outer Mn by displaying $A_1(\omega)$, defined in a manner similar to $A(\omega)$, except the spatial sums are now confined to the outer Mn . Similarly, $A_2(\omega)$ is the absorption spectrum of the inner Mn . We have found that we can only extract linewidths meaningfully from our simulations if we isolate the optical and acoustical modes by the procedure outlined earlier in this section. Of course, this cannot be done from experimental FMR spectra. In Fig. 8(b), we show the variation of the linewidths of the two modes with ω_1 . We see that ω_1 is decreased from the value 2 toward unity, the optical mode linewidth indeed approaches that of the acoustical mode, but then when ω_1 comes close to 1, the linewidths diverge. The acoustic mode narrows, and the optical mode broadens, as we have seen for the calculations presented earlier where ω_1 was taken to be unity.

IV. FINAL COMMENTS

In this paper, through analysis of spectral densities calculated at zero wave vector, we have extracted linewidths of the FMR modes of the structures we have explored. The origin of these linewidths, which are built into the theoretical methodology we have presented in the earlier paper, is in the spin pumping mechanism discussed elsewhere in the literature. We have seen that we obtain an excellent account of the linewidths reported in Ref. [6] for Fe Mn s on Au(100), and we also obtain a very good description of the quantum oscillations in linewidth reported in Ref. [14], for both the acoustical and optical modes of ferromagnetic trilayers grown on the Cu(100) surface.

These calculations employ the same theoretical methodology that we have developed and applied earlier to the analysis of the SPLEED data reported in Ref. [17]. In the SPLEED measurements, of course, it is large wave vector spin excitations that are studied. In Ref. [16], we obtained an excellent account of the dispersion of the single, broad asymmetric feature seen in SPEELS, along with an excellent account of both its width and asymmetric lineshape. Thus, the calculations presented in the present paper show that our method accounts very nicely for the damping of spin motions in these ultrathin Mn s throughout the two dimensional Brillouin zone, from the zero wave vector excitations explored in the FMR experiments to the large wave vectors probed by SPEELS.

It is interesting to offer a physical viewpoint of the FMR linewidths calculated here that is somewhat different (but complementary to) that set forward in papers devoted specifically to FMR linewidths. First, suppose we were to consider the FMR linewidth in an infinitely extended, three dimensional crystal described by a model such as we use here, in which electron energy bands result from interactions of electrons with the crystal potential, and ferromagnetism is driven by Coulomb interactions between the electrons. The FMR mode is the infinite wavelength, or zero wave vector mode of the system. Since such a Hamiltonian is form invariant under rigid rotations of the spins, the Goldstone theorem requires the linewidth of the zero wave vector mode to be identically zero. This is a rigorous statement, independent of approximations used in any specific calculation to study spin waves. Our mean field description of the ground state combined with the RPA description of the spin dynamics, is a conserving approximation and thus all of our conclusions are compatible with the Goldstone theorem. At zero field we will then find a width of identically zero, for the zero wave vector spin wave of the infinitely extended crystal. In real materials, of course, there is a finite width to the FMR mode, described phenomenologically by the damping term in the well known Landau Lifschitz Gilbert equation. The origin of the linewidth in real materials is the spin orbit interaction, since its introduction into the Hamiltonian produces a structure no longer invariant under rigid body rotations of all spins in the system.

Now when we place a thin ferromagnetic Mn on a non magnetic substrate, as in the systems considered here,

translational symmetry normal to the surface is broken, and only the components of wave vector parallel to the surface remain good quantum numbers. The lowest lying mode with $Q_k = 0$ is the FMR mode. This is not a uniform mode of the system, by virtue of the breakdown of translational symmetry normal to the surfaces; the amplitude of the spin motion in the non magnetic substrate differs from that in the ferromagnetic film, for instance. Hence, even in the absence of spin orbit coupling, one realizes a finite linewidth for this mode. This is a way of viewing the "spin pumping" contribution to the linewidth. Now in the limit that the thickness of the ferromagnetic film becomes infinite, the FMR mode of the film must evolve into the uniform mode of the infinite crystal whose linewidth must vanish in the absence of spin orbit coupling. Hence the spin pumping contribution to the linewidth falls to zero, with increasing ferromagnetic film thickness.

Other questions will be interesting to explore. Our method will allow us to explore the wave vector dependence of the linewidth, for example. Studies of this issue and other questions are underway presently.

Acknowledgments

During the course of this investigation, we have enjoyed stimulating conversations with Prof. B. Heinrich and with Prof. K. Baberschke. This research was supported by the U.S. Department of Energy, through Grant No. DE-FG 03-84ER-45083. A.T.C. and R.B.M. also received support from the CNPq, Brazil. A.T.C. also acknowledges the use of computational facilities of the Laboratory for Scientific Computation/UFLA.

-
- ¹ For instance, see the discussion of linewidths presented by B. Heinrich, page 195 of *Ultrathin Magnetic Structures II*, edited by B. Heinrich and J.A.C. Bland (Springer Verlag, Heidelberg, 1994).
 - ² R. Arias and D.L.Mills, *Phys. Rev. B* 60, 7395 (1999), *J. Appl. Phys.* 87, 5455 (2000).
 - ³ J. Lindner, K. Lenz, E. Kosubek, K. Baberschke, D. Spoddig, R. Meckenstock, J. Pelzl, Z. Frait, and D.L.Mills, *Phys. Rev. B* 68, 060102(R), (2003).
 - ⁴ S.M. Rezende, A. Azevedo, M.A. Lucena, and F.M. Aquir, *Phys. Rev. B* 63, 214416 (2001).
 - ⁵ D.L.Mills and S. Rezende, page 27 of *Spin Dynamics in Confined Magnetic Structures II*, (Springer Verlag, Heidelberg, 2002).
 - ⁶ The first experimental study was reported by R. Urban, G., Woltersdorf and B. Heinrich, *Phys. Rev. Lett.* 87, 217204 (2001).
 - ⁷ L. Berger, *Phys. Rev. B* 54, 9353 (1996).
 - ⁸ J. Slonczewski, *J. Magn. Magn. Mater.* 195, L261 (1999).
 - ⁹ E. Simanek and B. Heinrich, *Phys. Rev. B* 67, 144418 (2003).
 - ¹⁰ D.L.Mills, *Phys. Rev. B* 68, 014419 (2003).
 - ¹¹ E. Simanek, *Phys. Rev. B* 68, 224403 (2003).
 - ¹² Y. Tserkovnyak, A. Brataas, and G.E.W. Bauer, *Phys. Rev. Lett.* 88, 117601 (2002), and *Phys. Rev. B* 66, 224403 (2002).
 - ¹³ M. Zwierzycki, Y. Tserkovnyak, P.J. Kelly, A. Brataas and G.E.W. Bauer, *Phys. Rev. B* 71, 064420 (2005).
 - ¹⁴ K. Lenz, T. Tolinski, J. Lindner, E. Kosubek and K. Baberschke, *Phys. Rev. B* 69, 144422 (2004).
 - ¹⁵ R.B.Muniz and D.L.Mills, *Phys. Rev. B* 66, 174417 (2002), A.T.Costa, R.B.Muniz and D.L.Mills, *Journal of Physics (Condensed Matter)* 15, S495 (2003), *Phys. Rev. B* 68, 22414 (2003), and *Phys. Rev. B* 70, 54406 (2004).
 - ¹⁶ A.T.Costa, R.B.Muniz and D.L.Mills, *Phys. Rev. B* 70, 54406 (2004). We direct the reader to Fig. 3 for a comparison between experiment and the theoretically calculated linewidth and lineshape of large wave vector spin waves, for an eight layer Co film on Cu(100).
 - ¹⁷ R. Volmer, M. Etzkorn, P.S. Anilkumar, H. Ibach, and J. Kirschner, *Phys. Rev. Lett.* 91, 147201 (2003).
 - ¹⁸ Quite a number of authors use an adiabatic approach to calculate effective exchange couplings between nearby spins in ultrathin ferromagnets, then generate spin wave spectra utilizing a Heisenberg Hamiltonian appropriate to localized spins. In this picture, for a given wave vector in the surface Brillouin zone, one realizes N spin wave modes, each with infinite lifetime, with N the number of layers in the film. The calculations reported in ref. [15] and ref. [16] show that the adiabatic approximation breaks down qualitatively for ultrathin ferromagnetic films, and the picture of spin excitations just described is qualitatively incorrect. Instead, through most of the surface Brillouin zone, save for the near vicinity of the point, our theory predicted that one has a single, broad feature in the frequency spectrum of spin fluctuations, which displays dispersion with wave vector similar to that associated with a single spin wave branch. This picture is confirmed by the data reported in Ref. [17], and in Ref. [16] we demonstrate our approach provides a fully quantitative account of the data. An explicit comparison between adiabatic or Heisenberg like calculations, and our full dynamical calculations see Fig. 4 and Fig. 5 of Ref. [16].
 - ¹⁹ H. Tang, M. Plihal and D.L.Mills, *J. Magn. Materials and Magnetism* 187, 23 (1998).
 - ²⁰ MPIC is a portable implementation of MPI. See <http://www-unix.mcs.anl.gov/m pi/m ich>.
 - ²¹ MPI is a message passing interface standard. See <http://www-unix.mcs.anl.gov/m pi>.

²² R. B. Muniz and D. L. Mills, Phys. Rev. B 68, 224414 (2003).

²³ J. Mathon, M. Villeret, A. Um erski, R. B. Muniz, J. d'A buquerque e Castro, and D. M. Edwards, Phys. Rev. B 56, 11797 (1997).

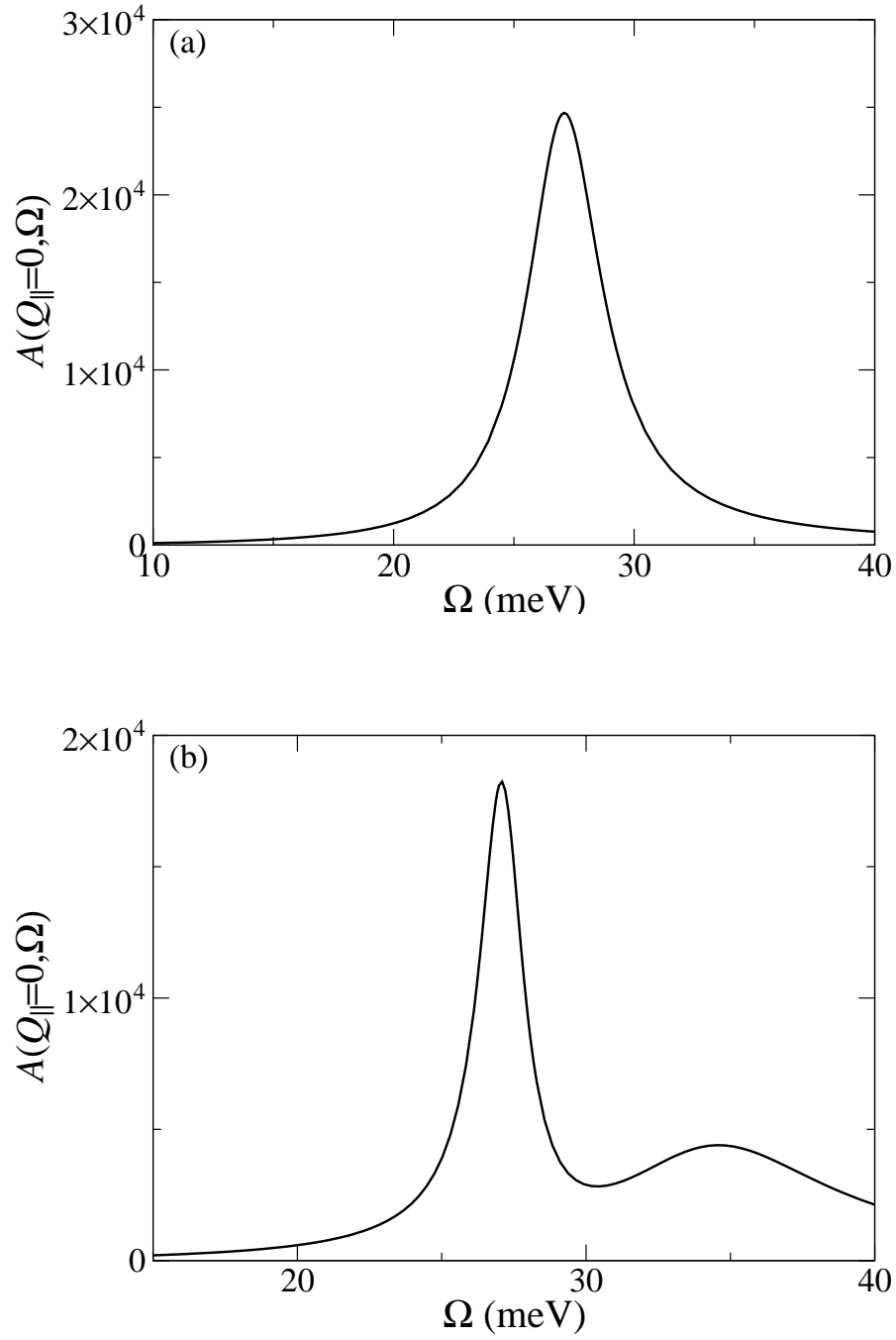


FIG. 1: We plot the spectral density function $A(Q_k = 0; l_z)$ for two cases: (a) a two layer Co_2Mn adsorbed on the $\text{Cu}(100)$ surface, and (b) a trilayer consisting of two Co_2Mn separated by two layers of Cu , with the complex adsorbed on the $\text{Cu}(100)$ surface. Each of the Co_2Mn has two layers. The Zeeman energy has been taken to be $\epsilon_0 = 2 \times 10^{-3}$ Rydbergs. Here l_z is chosen to be the innermost atomic layer of the magnetic structure.

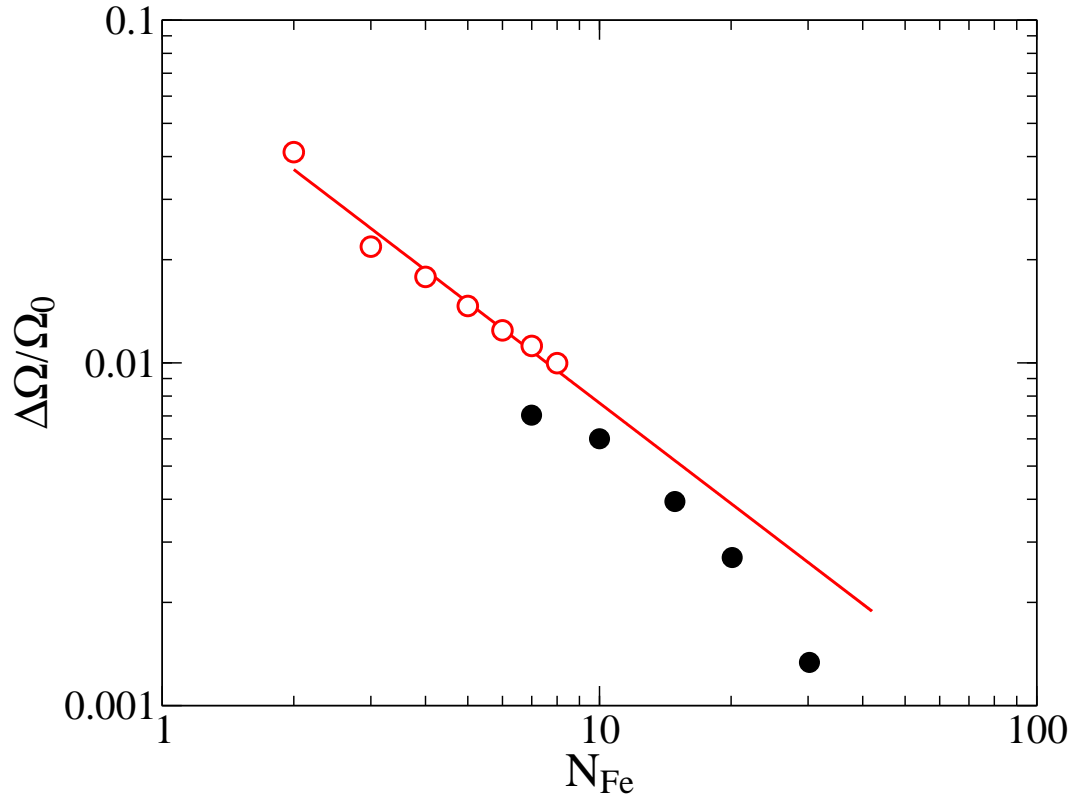


FIG. 2: For an Fe film on the Au(100) substrate, we plot the ratio $\Delta\Omega/\Omega_0$ as a function of N_{Fe} , the number of Fe layers. The results of the calculations are given as open circles, and the solid line is the best power law fit to the data, which is $1/(N_{\text{Fe}})^{0.98}$. The solid circles are taken from measurements reported in Ref. [6].

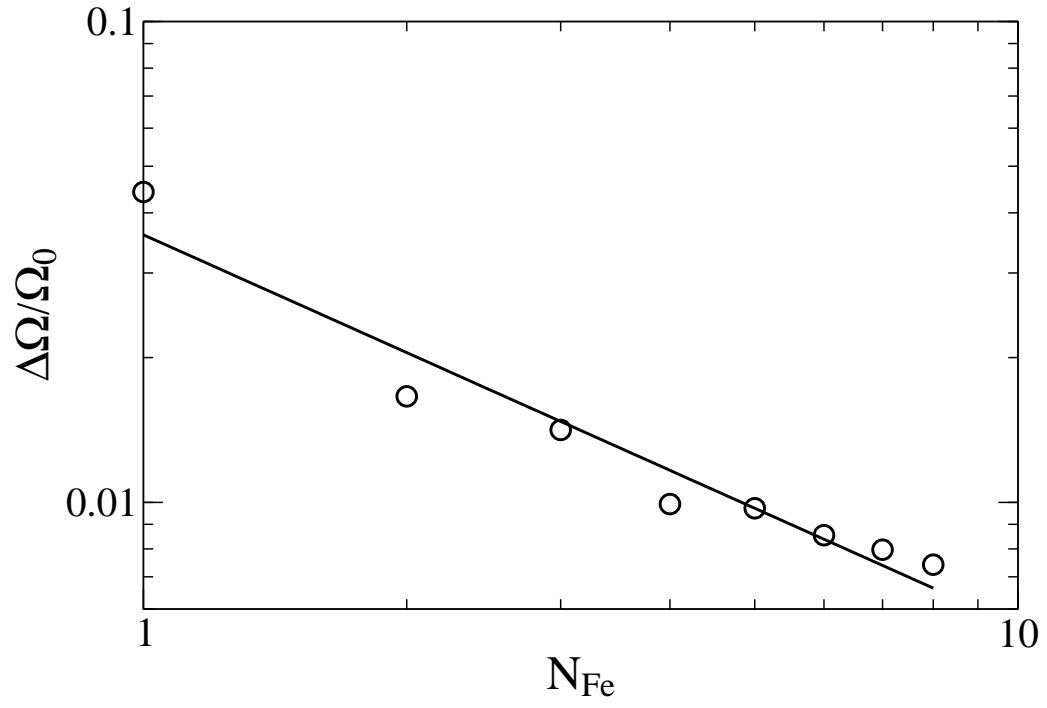


FIG. 3: The ratio $\Delta\Omega/\Omega_0$, for an Fe \ln adsorbed on the W (110) surface. The straight line is a best power law fit to the calculations, and gives a fall off with \ln thickness of $1/(N_{\text{Fe}})^{0.81}$. Clearly quantum oscillations such as discussed in Ref. [10] are present for small \ln thicknesses, so the power law fit is an oversimplification.

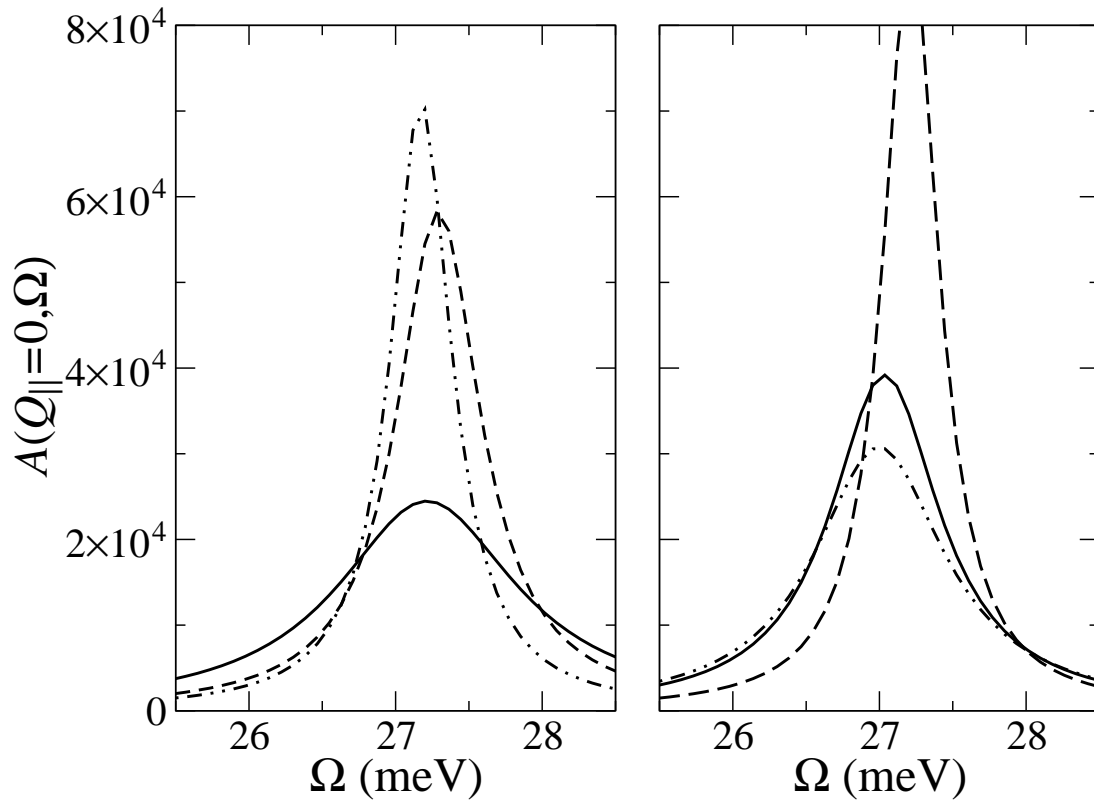


FIG. 4: For a two layer Fe film on Cu(110) (left panel) and for such a film on W(110) (right panel), we show how the linewidth is influenced by various coupling across the interface. In both cases, the solid curve shows the spectral density function generated by a complete calculation. The dashed curve has the d-d hopping terms across the interface set to zero, whereas the dot dash curve has the sp-sp hopping terms turned off.

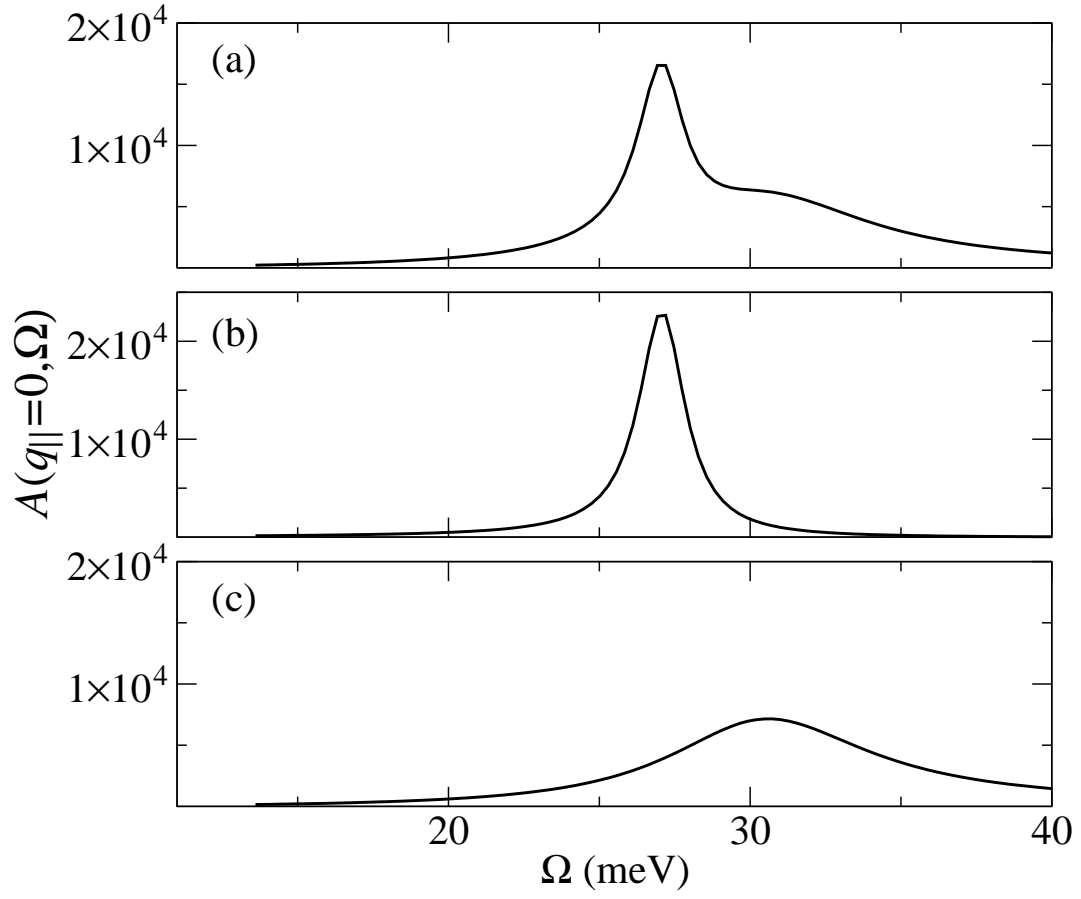


FIG. 5: For a $\text{Co}_2\text{Cu}_4\text{Co}_2/\text{Cu}(100)$ structure, we show (a) the spectral density function $A(0; \cdot; l_{\text{perp}})$, for the case where l_{p} is chosen to be the innermost layer of the inner Co_2 . Then in (b) we show the acoustic mode profile, where the mode has been isolated by the procedure described in the text. In (c), we display the optical mode.

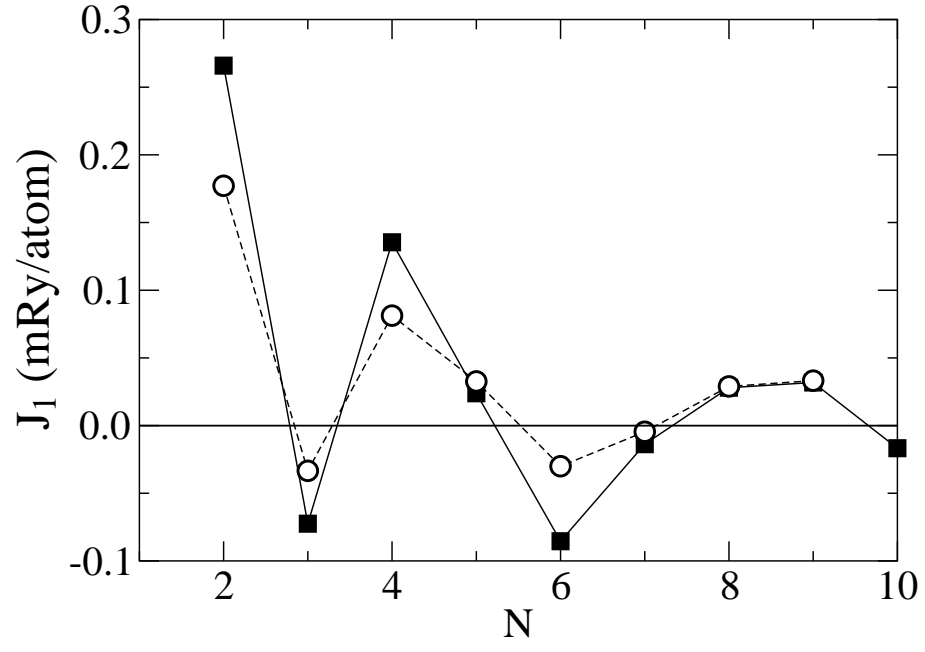


FIG . 6: For a $\text{Co}_2\text{Cu}_N\text{Co}_2/\text{Cu}(100)$ structure, we compare inter layer couplings deduced from our dynamic calculations of the splitting between the optical and acoustic mode of the trilayer (open circles, dashed line) with that calculated by adiabatic theory (solid circles, solid line).

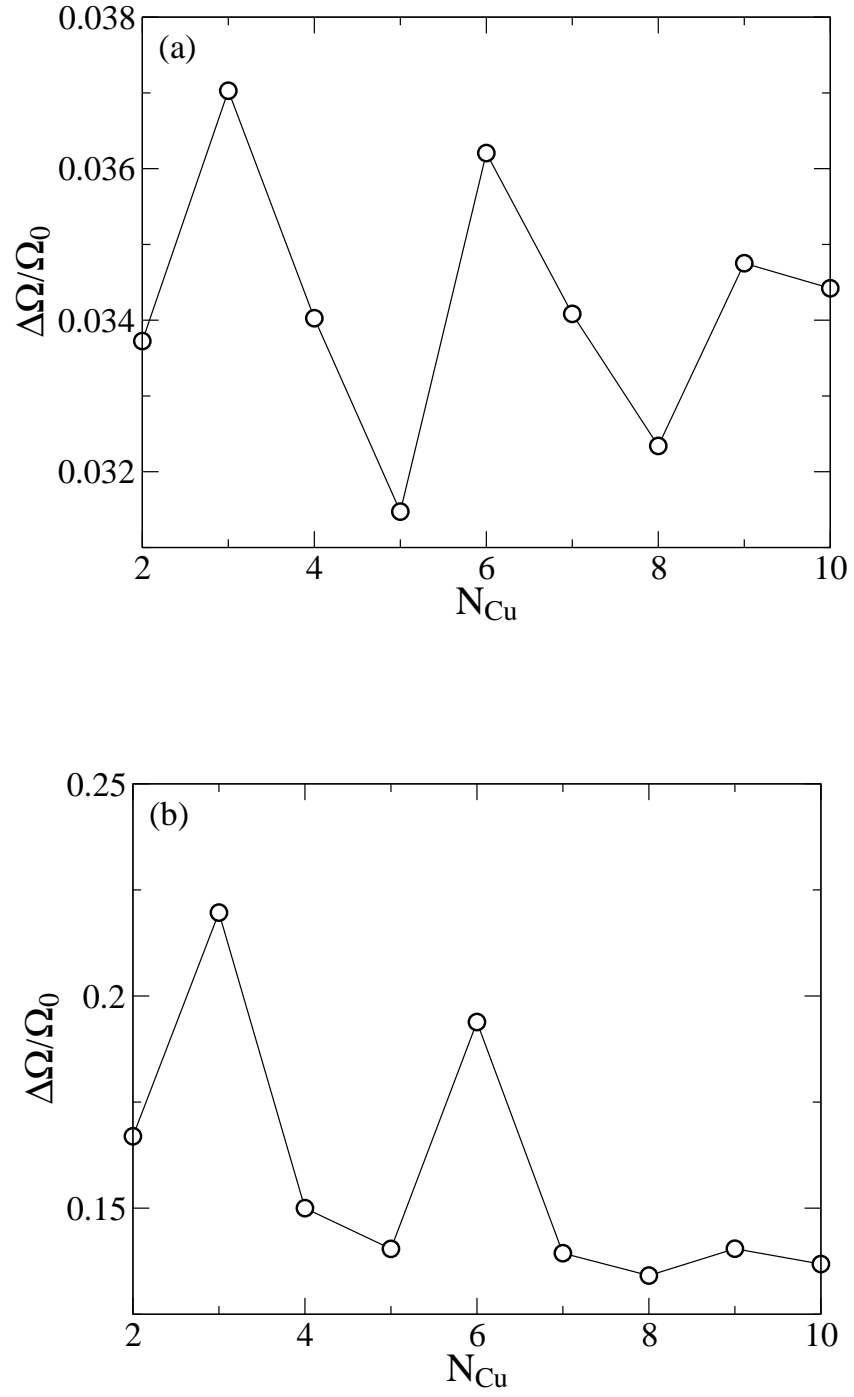


FIG . 7: For a $\text{Co}_2\text{Cu}_N/\text{Co}_2/\text{Cu}(100)$ trilayer, we show the variation with N of the linewidth for (a) the acoustic spin wave mode of the structure, and (b) the optical spin wave mode of the structure.

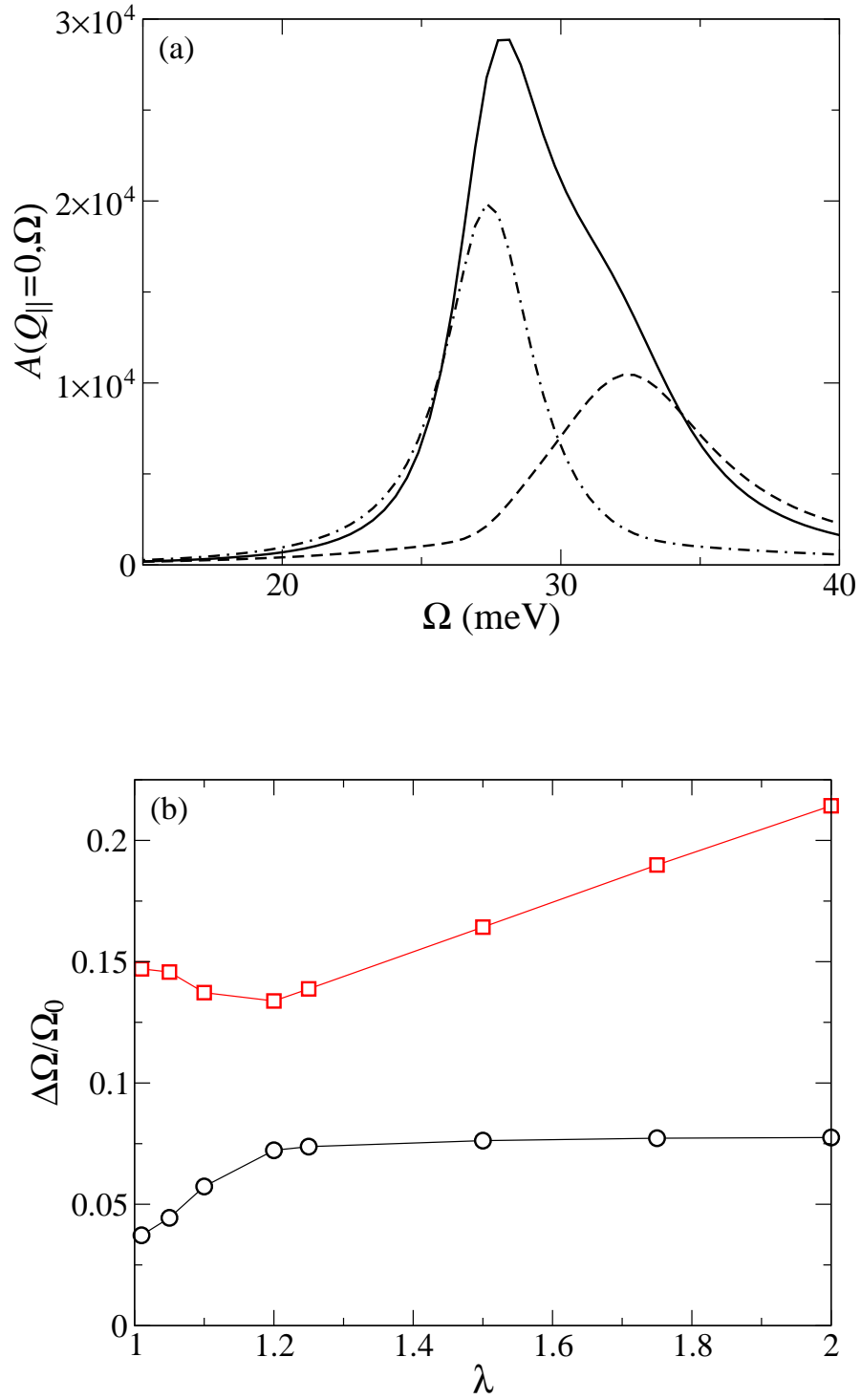


FIG. 8: This figure gives information on the spectrum of a $\text{Co}_2\text{Cu}_{10}\text{Co}_2/\text{Cu}(100)$ structure, where the frequency of the outer Ω_0 is 0 and that of the inner Ω_0 is Ω_0 . In (a), for the case where λ is 1.2, we show with the solid line the spectral density function $A(\omega)$ defined in the text. The dashed line is the spectral function $A_1(\omega)$ and the dot dash line is $A_2(\omega)$. In (b) we give the line width of the acoustical and optical modes of the trilayer as a function of the parameter λ .